ISSN: 2249-7196
IJMRR/ Dec 2021/ Volume 11/Issue 4/-/10-23
Nour Khlaifat / International Journal of Management Research & Review

Computational Fluid Dynamics modeling is used to examine the effects of various variables on the efficiency of horizontal wind turbines.

Nour Khlaifat, Ali Altaee*, John Zhou

Centre of Green Technology, University of Technology Sydney, NSW 2007, Australia

Abstract: The use of renewable energy sources as a substitute for conventional power plants that rely on fossil fuels and nuclear fuels is gaining a lot of attention. Wind energy is one of the most widely adopted renewable energy sources, with installations in a number of nations. Variables in the horizontal axis wind turbine's aerodynamic properties and layout abound. Environmental factors, blade shape, airfoil arrangement, and tip speed ratio are only few of the main sensitive aspects discussed in this work that impact the aerodynamic performance of the horizontal wind turbine. Computational Fluid Dynamics (CFD) modeling is used to estimate the flow around a horizontal wind turbine, and this article discusses the many turbulence models that may be used for this purpose. Lastly, the difficulties and final thoughts for future research paths in wind turbine design are presented.

Keywords: Keywords: airfoil; performance; turbulence model; Computational Fluid Dynamics; horizontal-axis wind turbine (HAWT) (CFD)

1. Introduction

As the global population and economy develop, so does the need for more energy [1]. By 2040, it is expected that global energy consumption would have increased by 56%, from 2010 levels of 524 quadrillion BTUs to 2040 levels of 820 quadrillion BTUs [2]. Large-scale use of fossil fuels is the leading cause of atmospheric carbon dioxide levels. CO2 emissions from the combustion of fossil fuels are expected to rise from 1 billion metric tons in 2010 to 36 billion metric tons in 2020, and maybe 45 billion metric tons by the end of 2040 [3].

Environmental consciousness, a reduction in the use of conventional fuel sources, and stringent environmental legislation have all contributed to a substantial and quick increase in the demand for clean energy sources [4]. Wind energy looks to be one of the most attractive emerging technologies owing to its cheap price and rapid worldwide expansion [5]. In 2013, there were 296,581 MW of installed wind power throughout the globe; by the end of 2018, that number had risen to 597,000 MW, and projections put it at 817,000 MW by 2021 [3].

Figure 1 displays the installed capacity of wind energy worldwide from 2007–2018 as reported by the Global Wind Energy Association. This figure is somewhat lower than the installed capacity of wind energy in 2017, which was roughly 50.1 GW (a). In 2017, the world's wind power capacity reached its third highest annual installation level ever, behind only 2015 and 2014. Yet, as shown in Figure 1, 2018's market growth rate of 9.1% was the lowest it has been since the advent of modern wind turbines in the early 1900s (b). Figure 2 [3] shows that in 2018, the top three nations contributing to wind turbine energy were China (34.81%), the United States (16.48%), and Germany (10.41%).

Figure 1. (a) New Installed capacity of wind energy and (b) Growth rates of wind energy.

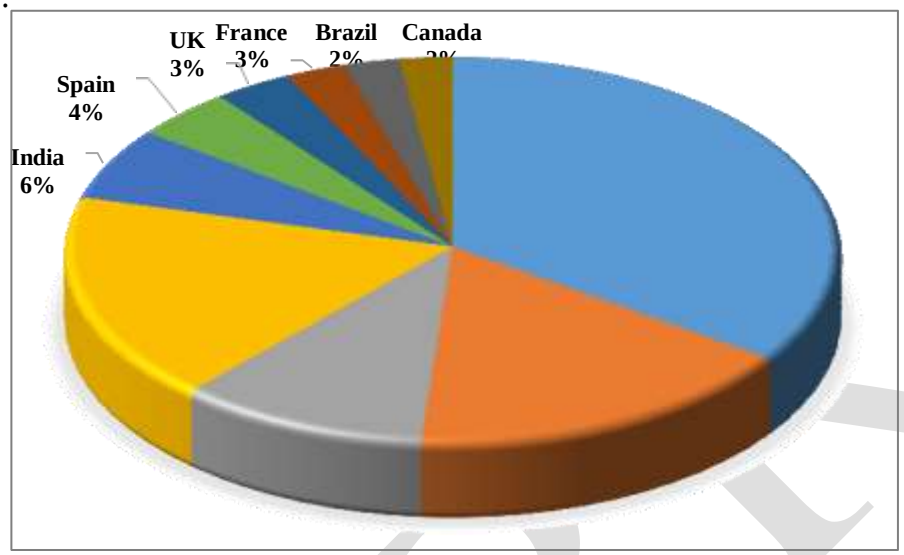

Figure 2. The percentage share of countries in the worldwide wind energy market at the end of 2018.

2. Few synthesis studies have been published on the topic of wind turbines. Lydia et al. [6] reviewed the modeling of power curves from wind turbines using several methodologies. Wind turbine monitoring approaches were surveyed and categorized by Tchakoua et al. [7], who also discussed recent advances and looming challenges in the field. Infield and Freris [8] examined the impact of wakes on downstream turbines from a fluid dynamics perspective. The study's objective is to highlight the significance of the elements that affect the aerodynamic efficiency of horizontal wind turbines. A wind turbine's ability to generate a given amount of electricity is very sensitive to a small number of details on how it is run. Optimization of wind turbine operating parameters is crucial for increasing the amount of power produced. Meteorological conditions (wind data models), wind turbine blade design, wind power curve/tip speed ratio, and airfoil shape are discussed. In addition, the study evaluates CFD models used to deal with flow concerns close to wind turbines.

3. Beginning with an examination of how horizontal wind turbines' aerodynamic qualities and the elements that affect them most directly, the essay progressed to examine the aforementioned sensitive factors. It also highlighted the various turbulence models and their applications via an examination of the aerodynamic properties of the horizontal wind turbine using CFD modeling.

4. Sensitive parameters of the aerodynamic performance of the horizontal wind turbine

4.1. Many variables, including climate and wind blade shape, influence HAWT's aerodynamic performance. The energy output of a wind turbine is proportional to the length of its blades. Knowing the most critical operational elements that affect the wind turbine's performance is essential for designing for the expected power output. Here, we'll go through the fundamentals of wind turbine construction and operation.

4.2. Atmospheric conditions (wind data models)

As the wind is the wind turbine's principal source of energy, its efficiency is directly related to the wind's speed. The average yearly, seasonal, and daily wind speeds differ at every given location. Thus, it is essential to characterize these differences using various mathematical distribution models [9]. In order to convince interested parties to increase or at least evaluate their investment in wind energy technology, it is crucial to conduct a thorough study of wind data. A probability distribution

function and other statistical approaches were presented for assessing the potential of wind resources in a given area.

Probability density functions characterize the frequency with which wind speeds occur. The probability distribution of wind speed has been modeled using both nonparametric and parametric techniques. Wind data analysis relies heavily on nonparametric kernel density estimation. Without resorting to parameter estimation of a theoretical distribution, kernel density estimators immediately reap the benefits of sample data. The distribution is given by the following equation:

where v is the wind speed in meters per second and v is the mean wind speed during a certain time interval. Probability study of wind speeds often makes use of the Weibull distribution function. Based on Eq. 2, we can see that the Weibull probability function is sensitive to two variables—scale and shape factor [11,12]:

$$(v) = \left(\frac{k}{c}\right)\left(\frac{v}{c}\right)^{k-1} e^{-\left(\frac{v}{c}\right)^{k}}$$

where $\boldsymbol{k}$ is the shape factor (dimensionless), and $\boldsymbol{c}$ is the scale factor (m/s). The curvature of the probability distribution function is decided by the shape parameter; any variation in the shape parameter is affected by the estimated wind potential. The Rayleigh distribution is employed when the mean wind speed is only available for the location. Rayleigh distribution is a special type of Weibull distribution when the shape factor is equal to 2, and the scale parameter depends on the mean wind speed. More spread of wind speed probability functions is related to a lower shape factor [13].

Determination of the Weibull function requires defining the shape and scale parameters, using different estimation methods. Using the maximum likelihood method, which is a widely accepted formula for defining shape and scale parameters is articulated in the following equations [14,15]:

$$k = \left(\frac{\sum_{i=1}^{n} v_i^{k} \ln(v_i)}{\sum_{i=1}^{n} v_i^{k}} - \frac{\sum_{i=1}^{n} \ln(v_i)}{n}\right)^{-1} \quad (4)$$

$$c = \left(\frac{1}{n}\sum_{i=1}^{n} v_i^{k}\right)^{\frac{1}{k}} \quad (5)$$

where v_i is the wind speed at time and n is the number of readings of wind speed data. To define the annual energy production of a wind turbine *(AEP)*, probability density distribution (v) is combined with the power curve of wind turbine $P(v)$ as shown in the following equation:

$$AEP = \int_{v_{cut-in}}^{v_{cut-out}} (v)\, f(v) dv$$

where v_{cut-in} is the cut-in wind speed (m/s), and $v_{cut-out}$ is the cut-out wind speed (m/s).

In the energy market, the values of wind speed at different hub heights of the wind turbine are very desirable, according to unavailable recorded data from wind station measurements. To calculate the wind speed *v(h)* at different altitude values *(h)* which depend on the measured wind speeds at reference value using power exponent law, the following equation [16] is proposed:

$$(h) = v_o \left(\frac{h}{h_{ref}}\right)^{\alpha} \quad (7)$$

where v_o is the wind speed at reference height (h_{ref}), and α is a power-law exponent (dimensionless) which varies with time of the day, terrain nature, temperatures, and season of the year [17]. The power-law exponent varies from 0.1 in smooth terrains to 0.40 in very rough terrains where a value of 1/7 could be used when no information about specific site formation.

Different studies have analyzed wind data using Weibull and Rayleigh probability distributions functions. For example, Islam et al. [18] assessed the potential of wind energy at Kudat and Labuan, Malaysia using Weibull distribution; their results confirmed the unsuitability of these sites for commercial wind energy generation. Krenn et al. [19] studied wind data in Austria over a ten-year period, depending on station data combined with a hybrid geostatistical model. The result indicated the feasibility of Weibull distribution in capturing the average annual wind speed with 0.8 m/s standard deviation of error. Celik [20] evaluated the potential of wind energy on Turkey's Mediterranean coast based on Rayleigh and Weibull models. The results showed that the Weibull model gives better accuracy of the power density distribution compared to the Rayleigh model.

In contrast, the Weibull model gives an annual average error of around 4.9% compared with 36.5%for the Rayleigh model when compared to wind speed measured reading. Mentis et al. [21] used the daily wind speed at different sites in Africa for one year by Weibull and Rayleigh distributions. Results showed 5% differences along with the findings between Rayleigh and Weibull distribution, but the variation exceeded 100% at specific locations. As such, the Rayleigh model is not valid at those sites, especially on the country level, and it can be used for estimating wind energy probability on a continental level only.

4.3. The shape of the wind turbine blade

The number of blades in wind turbines varies depending on the design [22–24]. Currently, the 3-bladed upwind horizontal wind turbine is the most popular modern wind turbine design due to its system efficiency, stability, and the economic feasibility of the wind turbine system. A horizontal wind turbine consists of majors major components. The foundation component of the wind turbine is the tower, which holds the nacelle, while the nacelle contains the transmission system, generator, andcontrol systems. The transmission system transmits the mechanical torque from the rotor to the generator, which includes the gearbox and mechanical brake system [25]. The generator uses electromagnetic components to convert mechanical power into electrical power [26–29].

Meanwhile, the rotor component captures the wind power and converts it into mechanical

torque. The rotor contains the blade component attached to the nacelle by the hub. Different materials are used in the manufacturing of wind turbine blades such as carbon-hybrid and S-glass [30,31]. Various studies demonstrated that decreasing the rotor and nacelle weight will reduce manufacturing costs. It should be noted that this decrease has a dynamic aero-structural limitation, and balancing issues need to be considered in the design [32,33].

One of the most design parameters of the shape of the wind turbine is the determination of the airfoil chord length and twist angle distribution along the blade, as seen in Figure 3(a). Discrete radial stations along the blade have been used to describe the shape of the blade, as shown in Figure 3(b). The chord, c(r), and twist angle β(r), which is the angle between tip airfoil and the local airfoil, have been used to define the shape of the blade.

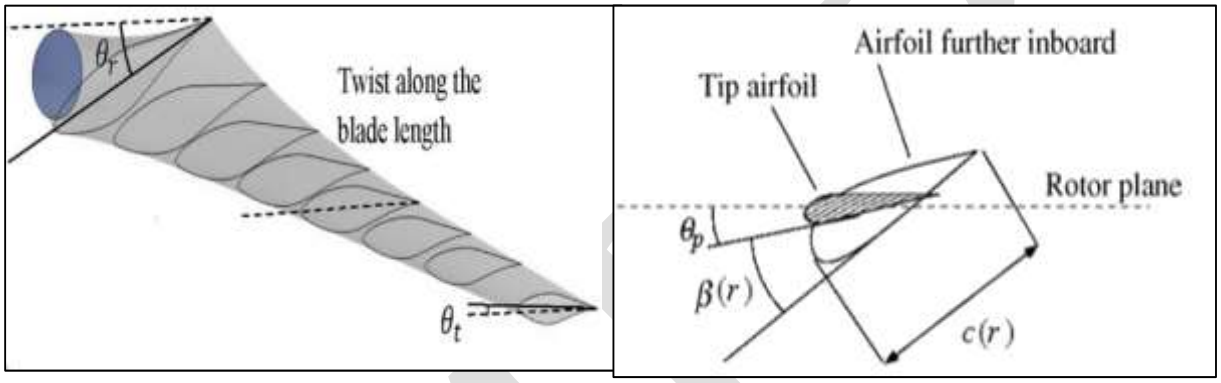

Figure 3. (a) Schematic of wind blade and (b) Sketch showing twist angle, chord lengthand pitch angle on a blade.

The distribution of airfoil chord length throughout the wind turbine blade is one of the most important design elements. Betz optimization theory is the simplest approach and provides reasonably approximation values of the chord length of the airfoil section, however there are other approaches [34]. When tip and drag losses are ignored, this approach yields a good optimal value of blade chord length with a tip speed ratio of 6-8. This approach is therefore erroneous in certain circumstances, such as when the tip speed is low, when the blade section is close to the hub, or when the airfoil portion has a high drag [35-37]. There are three main sections of a wind turbine blade: the root, the mid-span, and the tip. These sections serve different purposes in terms of both structure and airflow. Due to structural loads, the wider airfoil sections will be located at the tip region, while the wider chord length will be in the root area. Therefore, the initial torque is generated at the hub, whereas the majority of the production torque is generated towards the tip [38-42]. Studies have aimed to improve the wind turbine's aerodynamics.

By experimenting with varying twist angles and chord length distributions throughout the blade, researchers have found ways to improve the wind turbine's aerodynamic performance. The optimization's goal is to increase yearly energy production at a given site, where the wind potential is defined by the wind data model. Using a linearization of twist angle and chord profile approach, Liu et al. [43] investigated the innovative optimization of fixed speed wind turbines. After constructing an ideal blade with unique linearization for wind speeds between 4 and 7 m/s, they found a significant increase in yearly energy output. The rotor of a 300 kilowatt (kW) HAWT was designed using data from Semnan, Iran's wind speeds and the blade element momentum theory (BEM) [44]. Maximum power coefficient was considered together with manufacturing simplicity to determine the ideal wind turbine form. In a case study done in Iraq, Darwish et al. [45] found that the most appropriate wind turbine design could be chosen, laid out, and matched to increase the AEP in low wind speed zones. The blade geometry of a wind turbine was adjusted

by Al-Abadi et al. [34] using a gradient-based optimization approach called Blade Element Momentum (BEM). Using a computer analysis of a wind turbine, Derakhshan et al. [46] investigated the efficacy of the form optimization. According to their research, optimizing chords distribution boosted wind turbine output by 3.7% at rated speed (10 m/s) and by 1.2% on average across all wind speeds. In the Turkish wind farm of Gökçeada, blade optimization was performed by adjusting the twist angle and chord length of the blades.

The greatest AEP achieved was 92,972 kWhr, which is consistent with the concept [47].

4.4. Wind power curve and tip speed ratio

The power curve demonstrates how much energy can be generated by the wind turbine at various wind speeds. Improved grid planning and the ability to link wind energy to the power networks are the results of using this curve to predict wind speed [48]. For technical safety concerns, the turbine will shut down at the cut-out wind speed to minimize damage caused by excessive wind loads [49,50]. The cut-in wind speed is the minimum wind speed necessary to provide a usable power. Reducing the cut-in wind speed is one technique utilized to improve the HAWT's aerodynamic performance throughout a wide range of wind speeds. For instance, Singh et al. [51] used a numerical technique to build a wind turbine with improved start-up performance at low wind speed. This served two purposes: first, it lowered the cut-in wind speed, and second, it improved the lift-to-drag ratio. Using experimental data, this was shown to be correct.

In order to determine the optimal rotor size, the tip speed ratio must be taken into account. Tip speed ratio is the ratio of the rotor blade speed to the relative wind speed. Any deviation from a constant tip speed ratio may have a significant impact on the wind turbine's aerodynamic performance. So, if a rotor blade design is optimized for maximum wind speed, it will produce less torque at low wind speeds. This rotor's cut-in speed and self-starting challenges would also worsen while running in strong winds [24].

The output torque, mechanical stress and efficiency, aerodynamic characteristic, and noise [52] are only some of the design factors that should be considered when deciding on an optimum tip speed ratio. In practice, the noise pollution multiplies by a factor of six if the tip speed ratio is increased [53]. To get the best mechanical to electrical conversion from a contemporary three-blade wind turbine, the tip speed ratio should be six to nine, and from nine to ten for a two-blade wind turbine [54].

Table 1. Design consideration of tip speed ratio [52].

Tip speed ratio	Low (λ about 1, 2)	High (λ > 10)
Application	Traditional windmills	Single or two-bladed prototypes
Torque	Increases	Decreases
Aerodynamic stress	Decreases	Increases proportionally with arotational velocity
Efficiency	Decreases significantly belowfive due to rotational wake created by high torque	
Insignificant increases after eight		
Aerodynamics	Simple	Critical
Blade profile	Large	Significantly narrow
Noise	Increases to the sixth power approximately	

Pitch angle and generator torque are the primary operable performance factors in the HAWT. The generator's torque management mechanism will adjust the rotor speed so as to track the maximum power point. In contrast, with a pitch-regulated system, regulating the wind input torque will result in a power output that is consistent and quiet. As there is an optimal power coefficient linked to particular wind speed [55], the optimum power coefficient in pitch controlled variable speed horizontal wind

speed may be attained by controlling the ideal blade pitch angle and the optimum tip speed ratio.

4.5. Airfoil configuration

4.5.1. Conventional airfoil

Blades with optimal efficiency are constructed from several airfoil profiles that merge at a twisted angle and then taper to a circular blade root. Simplifying features including airfoil profiles, chord width, and twist angle are employed to streamline production in industry and save costs [56]. The torque produced by a wind turbine is highly dependent on the choice of airfoils. Aerodynamic performance of wind turbines is directly influenced by airfoil design. An important feature of the airfoil's aerodynamic properties is its lift to drag ratio. The lift and drag coefficients of airfoils with varying Reynolds numbers and angles of attack have been the subject of a number of experimental investigations during the last decade [57,58]. When determining an airfoil's drag and lift coefficients, the angle of attack is a crucial factor. Difference between flow angle and rotor plane angle used to get this angle's value. Thus, optimizing the lift to drag ratio [58,59] is the primary focus of wind turbine design.

At low angles of attack, where the lift coefficient is often significantly greater than the drag coefficient, a horizontal wind turbine's power production is primarily determined by the lift to drag ratio of the airfoil [57]. The design of contemporary wind turbines makes use of a wide variety of airfoil families, including those denoted by four- and five-digit NACA codes (e.g., NACA 65-415, NACA 63-215 [60]). The United States' National Advisory Committee for Aeronautics (NACA), the forerunner of NASA, is responsible for creating NACA. The NACA airfoils are best used at high Reynolds numbers and low angles of attack [61]. Among NACA families, the 63 and 44 series are the most well-known for their stall delay and reduced susceptibility to leading-edge roughness [62]. Ylmaz et al. [63] conducted an experimental study into the aerodynamic efficiency of the wind turbine blade and compared the findings to those obtained from a numerical simulation. Research examined the NACA 4420 airfoil and demonstrated that HAWT efficiency was determined by blade profile.

A second family, RIS-A-XX, is also utilized in the design of wind turbine blades; it was created and improved at the RIS National Laboratory in Denmark [64,66]. The form of the airfoil that is optimized using a B-spline representation is described using direct numerical optimization. There have been seven airfoils in this family, ranging in thickness to chord from 12% to -30%. Another set of airfoils is the DU series, which was created by researchers at the Delft University of Technology in the Netherlands. The thickness of a DU series airfoil, as measured in relation to its chord, may range from 15% to 40%, as shown in the examples of DU 91-W2-250 (25% of the chord) and DU 93-W-210 (21% of the chord) [67].

One family of airfoils utilized often in wind turbine design is the FFA airfoil family [60], which was created by the Swedish Aviation Research Institute. In further research, the S airfoil family has been designed by the National Renewable Energy Laboratory (NREL) [68,69]. Maximum lift-to-drag ratio, dynamic and structural requirements, and airfoil sensitivity to climatic variables are all factors that should be taken into account when choosing the airfoil used in wind turbines. Having a single airfoil profile that runs the length of a wind turbine blade has the opposite effect and makes the blade less efficient. Several airfoil forms may be utilized in the construction of a wind blade for certain purposes, however mixing between various airfoil shapes would improve efficiency.

According to structural load requirements [65], the root portion of an airfoil typically utilizes sections with a high thickness to chord length ratio. Yet, the lift-to-drag ratio is lower for thick-walled airfoils. Thus, a lot of effort has been put into finding ways to improve the lift coefficient of the thick airfoil typically used in wind turbine design. Using a narrow airfoil at the tip area is justified because of the importance of the aerodynamic characteristic in optimizing the lift to drag ratio.

Airfoils with a relative thickness of 25% or more are used in the inboard and mid-span sections of today's largest wind turbine blades. For inboard and midspan sections, for instance, airfoils like the FFA-W3-241 and FFA-W3-301 are utilized because of their comparatively large thickness [70]. The preferred airfoils for the wind turbine's tip area are the S809 and S814 [71], with blade lengths ranging from 10 to 15 m. Several research are looking at the performance of various airfoil families to see whether they can fulfill the aerodynamic and structural criteria for usage in wind turbine design. For instance, Van Rooij et al. [72] employed the Ris, DU, NACA, FFA, and S8xx airfoil families to do just that. The highest performing airfoils have a thickness to chord ratio of between 25% and 30%, including S814 (24%), DU 91-W2-250 (25%), and Ris-A1-24 (24%). Nonetheless, the DU 97-W-300 provides the highest overall performance for airfoils with a 30% thickness, given the constraints imposed by the design.

Maximum aerodynamic performance has been a central focus in recent blade designs for wind turbine rotors [73–75]. The amount of energy produced by a wind turbine changes when the wind changes speed and direction. Wind speeds are rather slow in many parts of the world. To address the energy demands of developing nations, there is extensive study into the creation of compact wind turbines. Aerodynamic features of airfoils utilized in wind turbines for places with wind speeds of 4-6 m/s were evaluated by studying lift, drag coefficient, and flow behavior of SG6043 at low Reynolds number by Ahmed et al. [76]. The lift coefficient was found to be relatively unaffected by freestream turbulence levels between 1% and 10%. Yet, the separation from the top surface was pushed back when the angle of attack was increased, which is indicative of a rise in lift and a fall in drag. The lift to drag ratio grows from 8 to 15 percent as the angle of attack increases due to the increased turbulence. The aerodynamic performance of many S-series was simulated by Sayed et al. [77] under moderate wind conditions. Based on the greatest lift to drag ratio they provide, the research determined that the S825, S826, S830, and S831 airfoils are the most effective in the S-series for low and high wind velocities.

Flow separation and other features of an airfoil change depending on the turbulence of the wind [78–80]. Delay flow separation from the airfoil's lift coefficient is also often used in models [81, 82]. Hoffmann [82] studied the results of increasing the wind turbulence intensity of NACA 0015 from 0.25 percent to nine percent at Re equal to two hundred fifty thousand. According to the results, the maximum lift coefficient increases due to the influence of delayed flow separation. It was found that changes in turbulence intensity had an effect on delayed flow separation and peak lift coefficient enhancement. At Re = 350,000, Kamada et al. [83] studied the dynamic and static features of DU93-W-210 at two distinct degrees of turbulence intensity. This airfoil, with a thickness of 21% relative, was tested in a wind tunnel with a turbulence grid to achieve a very turbulent flow. As the freestream intensity was increased, they found that the flow separation time slowed down, indicating that the stall angle of attack was greater.

4.5.2. Flatback airfoil

There have been many efforts to increase AEP by lengthening blades [84]. Manufacturers have also studied ways to shorten the blade by cutting down on the aerodynamic and structural stress [85]. Due to the high lift coefficient and bigger sectional area, flat back airfoils have been suggested for the inboard region of the blade to counteract the negative effects of the higher structural load brought on by longer blades [86,87]. The influence of increased structural stiffness and safety considerations on flatback airfoils, which have cross-section areas 20% bigger than those of non-flatback airfoils, was investigated by Kim et al. [88]. Furthermore, the decreased blade weight has led to a greater stiffness of the cross-section area [89,90].

Studies on the use of flatback airfoils in wind turbines have focused on a variety of aspects, such as the airfoil's aerodynamic properties, the design procedure, and the use of simulation tools [91–95]. While developing a flatback airfoil, Murcia and Pinilla [96] looked into the effects of various thicknesses and cutting techniques. Maximum lift and drag coefficients were shown to rise in both approaches, with the stall angle being the common denominator. Maximum lift coefficient is

increased by the thickness-adding approach compared to cutting methods. The flatback airfoil's design process was analyzed by Standish and Van Dam [97]. The research found that the flatback airfoil's aerodynamic performance might be enhanced by adding asymmetrical thickness to the baseline. So, the cutting procedure and the improvement of the aerodynamic properties of the airfoil are both aided by the combined addition of asymmetrical thickness to the design process.
A flatback airfoil for a high-output wind turbine was the subject of research by Law and Gregorek [98]. They determined that a flatback airfoil may achieve both a greater lift coefficient and a lower drag coefficient than a traditional airfoil. According to Homsrivaranon, the lift-to-drag ratio may be improved by using flatback airfoils, leading to improved aerodynamic performance. Flatback airfoils with ideal aerodynamic qualities were created by Chen et al. [99] using a genetic algorithm with two optimization targets (highest lift coefficient and greatest lift to drag coefficient). Improved lift-to-drag ratios were seen when a comparison of several numerical parameterization approaches to airfoil optimization was conducted by Zhang et al. [100]. Yet, the stall conditions have not improved. An increase in drag was seen due to base drag in the wake, which was experimentally confirmed by Baker et al. [101]. As compared to a standard airfoil, the lift coefficient increased when an asymmetrical thickness was added to the baseline, but the drag coefficient increased.

Increased drag at high angles of attack from separation vortices is one disadvantage of the flatback airfoil compared to a traditional airfoil [102]. As a flatback blade creates separation vortex around the hub in the spanwise direction, adding devices that inhibit separation vortex, such as a vortex generator, is an important area of study for improving wind turbine blades [103-105]. Ceyhan et al. [106] investigated the issue of flatback airfoils' greater drag coefficient, which restricts their structural applicability to inboard regions of the wind turbine's blade. As an alternative to traditional flatback airfoils, they proposed the swallowtail design. Their experimental results for the redesigned DU 97-300 flatback airfoil with a 10% thick trailing edge and no sallow tail supported their theoretical predictions. Results showed a 40% reduction in drag, meaning the wind blade's output power could be increased without altering how it was being used. As a result, the inboard section of wind turbines may benefit from the unconventional flatback. The flatback airfoil also has aero-elastic issues and increased noise from vortex shedding [107,108]. Nonetheless, a modest rise in rotor noise was produced by the inboard portion of the blade, where the flatback airfoil runs at speed lower than tip speed.

5. Computational Fluid Dynamic techniques

Commercial software like EllipSys3D and Fluent were utilized to solve flow issues near wind turbines using Computational Fluid Dynamics (CFD) methods in the early 1990s [109-111]. The lifespan of a wind turbine may be significantly affected by factors such as the wind's speed and direction. A thorough comprehension of the turbulence model, which represents the aerodynamics of wind flow around a wind turbine, is necessary for producing accurate results. Several types of turbulence models for the Navier-Stokes equations of fluid motion will be presented here. For each control volume cell, the equations of turbulence and momentum and mass conservation are solved using the finite volume approach in CFD methods.

5.1. Turbulence models

To yet, no one model has been able to accurately predict all of the physical properties of turbulent flow. Direct Numerical Simulation (DNS), Reynolds Averaged Navier-Stokes (RANS), and Large Eddy Simulation (LES) are only few of the models used to analyze the turbulent flow in wind turbines (LES). When it comes to determining turbulence, DNS provides the most precise results. Yet the time and money spent on calculation are substantial [112,113]. In order to solve the Navier-Stokes equations, RANS is the most often utilized model (see [114,115]). The mathematical principle notion relies on the Navier-Stokes equation's calculation approach, which separates the

flow into a fluctuating component and an average part using an equation known as the Reynolds decomposition. The RANS equation may be solved using a variety of turbulence models.

The eddy viscosity is determined by solving for two factors in the k- turbulence model series: the turbulent dissipation rate () and the turbulence kinetic energy (k). For simulating flows with separation phenomena, as the flow around a wind turbine at high wind speeds, the widely-used and widely-specified standard k- [116] produces unsatisfactory results. The Renormalization Group (RNG) k- and Realizable k- turbulence models [117,118] are extensions and refinements of the original k- model. Standard k- for turbulent kinetic energy (k) and dissipation rate () is used in both models, and their transport equations are identical. The models vary, however, in how they produce and calculate turbulent viscosity. The RNG k - turbulence model was solved statistically using the renormalization group theory. By taking into account the effect of rotation on eddy viscosity, for instance, the RNG k- turbulence is distinct from the normal k-. The RNG k- outperforms the traditional k- in predicting the flows of separations [119]. For rotating bodies, the realizable k- model is used because it has the potential to provide better results than the ordinary k- model for swirling flow issues within a narrow Reynolds number range [120].

Another extensively used RANS for wind turbine flow modeling is the k- turbulence model. It was Kolmogorov who initially presented the k- model [121]. Although the team at Imperial College has made some recent enhancements to the model, Wilcox's [122] work stands out as the most significant. Due to boundary layers having an unfavourable pressure gradient, the k- model is more accurate than normal k- in certain situations, and the sublayer may be incorporated without the need for additional damping functions. Yet, k- still has implementation limitations due to its sensitivity for certain flows with unconstrained stream borders. Ingeniously combining the benefits of the k- and k- turbulence models, Menter's [123] k- Shear Stress Transport (SST) is a state-of-the-art turbulence model. As a result, k- models are implemented in the lower levels of the boundary layer, with the transition to k- occurring gradually in the upper layers of the free shear layer and the wake area. Blending functions are involved in the translation between the two models. Modifying eddy viscosity to account for the influence of turbulent shear stress transfer is another strength of this model. Several adjustments to k- Shear Stress Transfer (SST) have been made to better rotation and streamline curvature [124].

The k- SST formed the basis for the extension that led to the transition SST (-Re) model, which is another RANS model [125]. It uses four transport equations, the first two of which are equivalent to the k- (SST) equations, and the third and fourth of which are the equations for the intermittency () and transition momentum thickness (Re), respectively. Since it accounts for the laminar-turbulent transition flow model in which flow and stall processes separate, the transition SST model is more accurate than traditional turbulence models.

In terms of RANS turbulence models, the Spalart-Allmaras (SA) is the simplest since it only requires one transport equation. In this case, one transport equation is used to compute the turbulence amount [126], and the kinematic eddy turbulent viscosity is the dependent variable. This model was developed and is best suited for aerospace applications involving a compressible flow across airfoils and wings. For instances with unfavourable pressure gradients, it may simply propose a new kind of grid, which becomes readily stable and converges to the solution [127]. Moreover, the model may allow for substantial diffusion, particularly in areas of 3D vortex movement [128]. Spalart and Shur [129] and Rahman et al. [130] have both done work to

ameliorate the situation by factoring in the impacts of rotation, being close to the wall, and decreasing the diffusion effect. The reduced calculation time of this model compared to previous turbulence models is a major benefit of its quick convergence [127].

As compared to the Direct Navier-Stokes model, the processing requirements of the alternative model known as Large Eddy Simulation (LES) are far lower. Deardorff [131-134] conducted the first experiment using LES in engineering. The RANS model is limited in its application, whereas the LES turbulence model provides more precise findings. One other perk of LES techniques is that they split turbulence into two portions in the computing domain, making it easier to reduce the length of scales involved. In the first, the crucially vast sizes were completely resolved, whereas in the latter, the little sub-grid scales were modeled. As compared to other turbulence models, LES models give a sufficient prediction of complicated flow [135,136]. This advantage is especially apparent in examinations of high Reynolds number turbulence models. However, the LES model takes longer to calculate than the RANS model does. The Detached-Eddy Simulation (DES) was developed in 1997 [137] and applied for high Reynolds number with a massively separated flow [138]. The latter method is a model that blendsthe LES and RANS approaches. Hence, LES is applied with external flow regions with massive separations, whereas the boundary layer is solved by RANS [139]. Travin et al. [140] described the DES as a single turbulence model that uses unsteady three-dimensional numerical methods. Johansen et al. [141] found that using DES approaches does not improve the characteristics of the wind turbine when using the DES method due to the required long computational time.

5.2. Application of turbulence models used for aerodynamic simulation of the wind turbine

While designing wind turbines, the accuracy of the numerical modeling of the flow around the turbine is highly dependent on the numerical models used. Many turbulence models have been published and used to check the accuracy of numerical approaches versus experimental studies. To investigate the unstable RANS and DES models, Li et al. [142] employed CFD Ship-lowa with a sliding mesh for NREL Phase VI. Thrust forces and moments were discovered to have different findings in the research compared to the experimental work. Yet, the turbulent flow of the wind turbine was significantly reduced by using DES.

The numerical modeling of NREL Phase VI using k- SST and transition SST has been explored by Lanzafame et al. [143], Potsdam and Mavriplis [144], and Rajvanshi et al. [145]. The experimental investigation showed that transition SST has superior capabilities than k- SST. Moshfeghi et al. [146] examined how a near-wall grid treatment affected the wind turbine's aerodynamic performance. Using k- SST and transition SST turbulence models, we analyzed the NREL Phase VI model for a near-wall grid with eight different scenarios. It is possible to calculate thrust forces and pressure coefficients using a range of wind speeds. Test findings for thrust values did not correlate well with the thrust force results of k- SST. The performance of the wind turbine is over-predicted by the k- SST model. Although though the results are similar to the experimental study, the transition SST behavior deviates from the k- SST model, especially in the inboard areas. The dynamic behavior of the flow around the wind turbine and the wake is investigated using k- turbulence models. Full-scale studies of three wind turbines using various k- turbulence models were conducted by Kasmi and Masson [147] and Abelsalam et al. [148]. This demonstrated that the improved k- model more closely matches prior experimental data. Many studies have compared the

efficacy of different turbulence models for forecasting wind turbine performance. The NREL Phase VI was calculated by Rutten et al. [149] using a pair of RANS models (k-, k- SST). While comparing the k- SST turbulence model to the k- model, it became clear that the former provides more accurate predictions of the turbulent kinetic energy value. Using RANS and 12 turbulence models, Abdulqadir et al. [150] looked at how well they could forecast the performance of the NREL Phase VI wind turbine. When compared to the experimental data, all of the RANS numerical key performance coefficients at low tip speed ratios were shown to have a high value. Nonetheless, k- SST obtained the worst simulation results at high tip speed ratios, whereas realizable k- highlighted rather acceptable outcomes.

In order to better estimate the aerodynamic features around the NREL Phase VI blade rotor, You et al. [151] looked into the impact of three distinct RANS turbulence models (Spalart-Allmaras, k- SST, and transition SST). Their findings confirmed that transition SST effectively captured laminar separation bubbles close to the airfoil and rotor blade. Due to its accurate prediction of the boundary layer's transition, the k- Transition model yields findings that are consistent with experimental evidence. area. An investigation into predicting the numerical performance of a New Mexico wind turbine looked at the effect of RANS turbulence models using two different near-wall methods of high and low Reynolds number [152]. The RANS models used in the high Reynolds model were the Spalart-Allmaras and *k-ε RNG*, while the models employed for low Reynolds number were *k-ω SST* and *k-ω* transition. All four models, under low wind speeds range, could predict well the wind turbine's aerodynamic performance. When the wind speeds increased, more differences between the models appeared, and the high Reynolds model had better results compared with the low Reynolds model. A swirl effect was considered with wall function corrections, where the *RNG k-ε* turbulence model is recommended when wind speed increases [152].

This section summarizes the benefits and drawbacks of each turbulence method. When it comes to turbulence solutions, DNS and LES are more accurate than RANS. However, a considerable amount of time and computing power is needed. Given the trade-off between accuracy and computing cost, RANS has emerged as the preferred method. Popular and frequently used standard k- provides poor modeling results for flows with separation phenomena, such as a wind turbine at high wind speed. While attempting to foretell separation flows, RNG k- is more reliable than traditional k-. As compared to the ordinary k- model, the results for swirling flow issues under certain Reynolds numbers are better in the realizable k- model. Nevertheless, the sensitivity of the k- model for flows with free stream boundary conditions limits its use to wind turbines, despite the fact that it is a simple model. In order to improve rotation and streamline curvature, k- Shear Stress Transfer (SST) was used in wind turbine flow issues. Since it accounts for the laminar-turbulent transition, when separation and stall events occur, the transition SST model is more accurate than traditional RANS turbulence models. The prior research on the CFD summary for HAWT is summarized in the following table.

6. Conclusion remarks and challenges

The authors suggested a future line of inquiry that might lead to fruitful findings: designing blades with environmental factors in mind. It is difficult to validate computational fluid dynamics (CFD) models without sufficient experimental data from wind turbines. Consequently, future efforts in CFD models should use actual wind speeds. Airfoil configuration, or the differences between conventional and flatback airfoils from an aerodynamic standpoint, is an area that the authors believe still needs further investigation. Wind turbine technology faces a number of obstacles, including, but not limited to, intense market rivalry [176], the unreliability of wind measuring instruments [177], difficulties in operation [178–183], and issues with electricity and grid

distribution [184–186]. Control system improvements [187,188] and wind prediction tools [189-191] may be attained via a variety of methods. Wind turbine aerodynamics have been researched for almost two centuries, with the majority of the research focusing on the difficulties encountered and the ways in which they were overcome via experimental means. The expense and difficulty of 3D simulation mean that the field is still in its infancy. In this study, we'll take a look back at the fundamentals of wind turbine aerodynamics. The most important takeaways from this analysis are:

• Precise information on the wind's dispersion is required for each individual site's wind turbine design. The occurrence frequency of a given wind speed is often calculated using one of two probability distribution functions: Weibull or Rayleigh. Several research have developed models to evaluate the reliability of these probability density functions. • The HAWT power curve, the tip speed ratio, and the blade plane form were all factors in the development of wind turbines. Reducing cut-in speed, selecting the right tip speed ratio, and keeping mechanical stress and noise in mind are just a few of the investigations that have been conducted to improve aerodynamic performance.

• The choice of airfoil in a contemporary wind turbine comes down to a number of factors, including the lift-to-drag ratio. To improve the effectiveness of wind turbines, researchers have experimented with different airfoil design criteria. Further study is needed in this area.

• The CFD simulation of HAWT is a great tool for estimating aerodynamic performance, with the accuracy depending on the use of appropriate turbulence models. The majority of ongoing numerical effort is dedicated to improving CFD models' ability to forecast aerodynamic performance. Cost and time limitations are addressed by use of simulated trials.

References

International energy forecast 2016 with predictions to 2040. 1. Conti J, Holtberg P, Diefenderfer J, et al. Federal Energy Regulatory Commission (FERC), Washington, DC (USA), 2016.

Two. Sims RE, HH Rogner, and K Gregory (2003) A look at how much different types of power generation—fossil fuel, nuclear, and renewable—cost in terms of carbon emissions and the cost to mitigate those emissions. The Journal of Energy Policy 31(9):1315-1326.

3. W. W. E. A. (February 25, 2019) (February 25, 2019) As of 2018, the global wind power capacity has increased by 50,1 GW, bringing the total to 597 GW.

Using the MOPSO algorithm, Kaviani H. and Nejat A. (2017) optimized the aeroacoustic and aerodynamic performance of a MW-class HAWT. Energia 140: 1198-1215.

5.Ashrafi, Z. N., M. Ghaderi, and A. Sedaghat. 2015. Parametric research on off-design aerodynamic performance of a horizontal axis wind turbine blade and suggested pitch control. Energy Conversion and Management 93:351-356.

Lydia M., S. S. Kumar, A. I. Selvakumar, and M. Kumar (2014) provide an in-depth analysis of the methods used to calculate power curves for wind turbines. Energy Sustainability 30(4-5):460.

Wind turbine condition monitoring: A state-of-the-art review, emerging trends, and future challenges. 7. Tchakoua P, Wamkeue R, Ouhrouche M, et al. Seven, 2595-2630, Energy.

Sanderse B, van der Pijl SP, Koren B. (2011). The aerodynamics of wakes created by wind turbines are examined via a computational fluid dynamics lens. Wind Power 14:799-819.

#9 Infield D, Freris L (2020). John Wiley & Sons, Renewable Energy in Electrical Systems.

Aerodynamic design and analysis of a 10 kW horizontal-axis wind turbine for Tainan, Taiwan. Bai CJ, Chen PW, Wang WC. 2016. 18(9), 1151-1166, Clean Technology and Environmental Policy.

Wind energy explained: theory, design, and application, by John F. Manwell, James G. McGowan, and Alan L. Rogers, John Wiley & Sons, 2010.

12, Katsigiannis YA, Stavrakakis GS (2014). Comparison of the technical and economic viability of

several kinds of wind turbines in estimating wind energy generation at a variety of Australian locales. Energy, 67(9), Renewable, 230-236.
Renewable and Efficient Electric Power Systems, GM Masters (2013), 13. A.M. Wiley & Sons, Inc.
Weibull parameters for wind energy production in the northeast area of Brazil: a comparison of seven numerical approaches. Rocha PAC, de Sousa RC, de Andrade CF, et al., 2012. Apl Energy 89: 395–400.
Weibull wind speed distribution for wind energy analysis: up-to-date parameter estimate by Seguro J and Lambert T, 2000. Journal of Wind Engineering and Industrial Aerodynamics 85:75-84.
Determining the surface roughness parameter and wind shear exponent of the Kisii Area using On-Site measurements of wind profiles. Laban ON, Maghanga CM, Joash K (2019). 2019 J. Environ.
Wang L, M. E. Cholette, A. C. Tan, et al (2017) An effective computational technique for optimizing the spatial configuration of actual wind farms, taking into account topographical differences between individual turbines. Energy 132: pp. 147-159.
Weibull distribution function for the assessment of wind energy potential in Kudat and Labuan, Malaysia, by Islam M, Saidur R, and Rahim N, 2011. Number 36, Issue: 985-992, on Energy.
19 Krenn, A., H. Winkelmeier, R. Cattin, and A. et al.
Available at www.windatlas.at/downloads/20101117 Paper Dewek.pdf.